Tight-binding study of ZnSe/ZnTe strained superlattices: Determination of the band offset from the optical properties

F. Malonga, D. Bertho, C. Jouanin, and J.-M. Jancu
Université de Montpellier II, Groupe d'Etude des Semiconducteurs, URA CNRS 357, 34095 Montpellier Cedex 05, France
(Received 16 March 1995)

We have theoretically studied large-, short-, and very-short-period ZnSe/ZnTe strained superlattices. We use an sp^3s^* tight-binding model with spin-orbit coupling in order to calculate energies of superlattice electronic states and optical transition probabilities. This enables us to estimate the valence-band offset considering many experimental studies on a large range of samples with various thicknesses and strain states. For large-period superlattices, our work evidences the important role of unconfined excited states in optical transitions and explains that low-energy structures observed in the absorption spectra are due to transitions between spatially separated conduction and valence superlattice confined states. The main absorption contribution at higher energy is explained by strong transitions occurring between valence and unconfined conduction states. These features result from the type-II nature of this superlattice. Our calculation leads to a 1.02 ± 0.02 eV unstrained band offset, which allows a very good comparison with the studied experimental data.

I. INTRODUCTION

In the last few years, II-VI semiconductors have attracted considerable interest as promising optoelectronic devices in the infrared and visible regions. The constant progress in epitaxial crystal-growth techniques allows the elaboration of structures which are good candidates for the realization of blue light emitters. The association of two different semiconductors in heterostructures broadens their application fields, and ZnSe/ZnTe superlattices are very interesting structures to tune wavelengths by variation of the thickness of the material layers. Up to now, these superlattices have been obtained by different growth techniques such as molecular-beam epitaxy (MBE),[1-4] atomic layer epitaxy (ALE),[5,6] hot wall epitaxy (HWE),[7,8] and metal-organic vapor-phase epitaxy (MOVPE).[9] A number of experimental results have been reported on these structures. Characterization studies reveal the good crystallographic quality of these superlattices, and the existence of well-defined interfaces. The main characteristic of ZnSe/ZnTe superlattices is the existence of a large mismatch of about 7.2% between the two host materials. This entails strong biaxial internal strains. As a result, ZnTe layers matched to ZnSe ($a_{ZnSe}=5.6676$ Å) experience a 4.7-GPa biaxial compression. Conversely, the biaxial dilation reaches 6.2 GPa within the ZnSe layers strained to the ZnTe ones ($a_{ZnTe}=6.1037$ Å). Moreover, the strain state of the superlattices is largely dependent on the nature of the substrate GaAs, InP, or other, and on the presence of buffer layers like ZnSe or ZnTe which are sometimes used. When the layer thickness exceeds the critical value, the strain distribution is deeply modified by creation of defects and misfit dislocations at the neighboring interfaces. The final strain state depends on the structure and is not always well known. Because of the large value of the mismatch, the induced strains cannot be maintained on thick layers, and the critical thickness beyond these defects that is created is small, only 1–2 nm. Two extreme cases can easily be characterized so long as the thickness of each layer is lower than the critical thickness. First, the superlattice thickness is large enough to allow the superlattice to take an equilibrium state independent of the substrate by creating a dislocation zone which accommodates the elastic energy. In this situation, usually referred to as free standing, the lattice constant in the direction parallel to the interface has the same value in all superlattice layers but differs from the lattice parameter of the substrate. In the second case, the superlattice is grown coherently on the substrate with the same lattice parameter in the whole structure substrate included. All of this shows that knowing the strain distribution in highly strained superlattices is a rather complex problem. A second important point in studies of ZnSe/ZnTe heterostructures is the band-offset value. Predicted values of the valence-band offset have been reviewed by Miles, McCaldin, and McGill[10] and more recently by Priester, Bertho, and Jouanin,[11] who have calculated band offsets at strained II-VI heterojunctions. The range of values is very large, extending from 0.36 up to 1.4 eV. Recent studies[12,13] suggest that the band offset could be near 1 eV, in agreement with previous predictions and the electronic affinity difference. However, some uncertainty still remains about the theoretical determination of the valence-band offset. In addition, the experimental results available for the ZnSe/ZnTe valence-band offset are sometimes contradictory. This may be due to the fact that the most of the works are based on indirect determinations such as photoluminescence measurements. In this kind of experiment, the determination is usually achieved by varying the valence-band offset in order to fit theoretical results with the first excitonic transition. However, such a determination makes sense only if the value is determined through a fit over a large range of

0163-1829/95/52(7)/5124(8)/$06.00

samples, with different thickness layers and for various states of strain. Moreover, this determination is made difficult by the interpretation of the observed photoluminescence peaks. The lower-temperature photoluminescence in ZnSe/ZnTe can have an extrinsic origin, as shown by Davies[14] and Yao *et al.*[15] These works suggested the extrinsic nature of these peaks in $ZnSe_{(1-x)}Te_x$ alloys and ZnSe/ZnTe superlattices, and proposed that it be attributed to the radiative recombination of excitons bounded on a single isoelectronic Te atom or on Te clusters located in ZnSe layers. To our knowledge, there are two theoretical approaches concerning the band structure of ZnSe/ZnTe superlattices. The first one[16] is based on second-order $\mathbf{k}\cdot\mathbf{p}$ theory with an eight-band model, and includes the effects of strain and spin-orbit splitting on the electronic band structure. Assuming that the nature of the first photoluminescence peak is extrinsic, the valence-band offset, determined by fitting $\mathbf{k}\cdot\mathbf{p}$ results to the peak energy measured on some samples[1,7] is 0.975 eV (1.196 eV in the case of intrinsic luminescence). In the second approach,[17] based on the semiempirical tight-binding method,[18] the energy-band gaps of short-period ZnSe/ZnTe superlattices are calculated. Assuming that the emission observed for ZnSe/ZnTe superlattices with periods of 2 nm originates from intrinsic luminescence, the comparison of theoretical predictions with experimental results of the photoluminescence emission peak energy[2] leads to a valence-band offset of 1.136 eV. Spin-orbit coupling has some effect on the electronic properties in strained systems, and is not considered in this calculation. For instance, without spin-orbit interaction, the variation of the light-hole band edge with uniaxial pressure is twice as great as with spin-orbit interaction. Moreover, the importance of band mixing at the zone center has been shown in highly strained heterostructures.[19,20] The parameters used in this method[17] are fitted to energy values at high-symmetry points of the Brillouin zone, and lead to an overestimate of the effective masses at the zone center. In addition, the deformation potentials which are essential in the determination of the electronic band structure of strained superlattices greatly deviate from the experimental values. This is shown in Table I, in which the uniaxial deformation potential at the zone center and effective masses obtained from Ref. 17 are compared to the experimental values. This affects the position of band edges in a non-negligible manner, and introduces uncertainty into the offset determination. Figure 1 gives the light- and heavy-hole band-edge positions between ZnTe and ZnSe according to the nature of the substrate (ZnTe or ZnSe). With our tight-binding parameters including spin-orbit coupling, the bottom of hole wells are always in ZnTe, whatever the substrate [Figs. 1(a) and 1(b)]. Within a description without spin-orbit coupling and a poor description of strain effect,[17] the heavy-hole well depth is changed by 200 meV, and the light-hole well depth by 900 meV [Figs. 1(c) and 1(d)]. The light-hole well is dramatically modified, and the bottom of the well is observed in ZnSe layers.

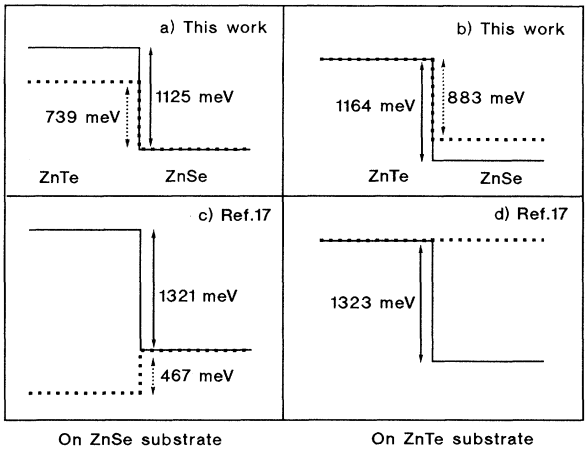

FIG. 1. Light-hole (dotted line) and heavy-hole (full line) band alignments between ZnTe and ZnSe. (a) This work with a ZnSe substrate. (b) This work with a ZnTe substrate. (c) Obtained from Ref. 17 with a ZnSe substrate. (d) Obtained from Ref. 17 with a ZnTe substrate.

In this paper a theoretical study of the electronic band structure of ZnSe/ZnTe superlattices using the tight-binding approximation is reported in order to estimate the valence-band offset, considering many experimental

TABLE I. Values of the uniaxial deformation potential b (in eV) and of the electron m_c, light-hole m_{lh}, and heavy-hole m_{hh} effective masses (in units of electron mass m_0) in the [100] direction.

	ZnSe			ZnTe		
	Others[a]	This work	Experiment	Others[a]	This work	Experiment
b (eV)	−3.2	−1.2	−1.2[b]	−3.41	−1.2	−1.2[c]
(m_c/m_0)	0.210	0.160	0.160[d]	0.117	0.172	0.130[e]
(m_{hh}/m_0)	−0.530	−0.495	−0.495[f]	−0.516	−0.398	−0.398[g]
(m_{lh}/m_0)	−0.150	−0.152	−0.152[f]	−0.107	−0.177	−0.177[g]

[a]Obtained from parameters of Ref. 2.
[b]Reference 24.
[c]Obtained from Refs. 36 and 37.
[d]Reference 25.
[e]Reference 37.
[f]Reference 34.
[g]Reference 38.

studies over a large range of samples with various thicknesses and strain states. This offset is due at once to strain effects and to the unstrained offset between the valence-band edges of the two unstrained bulks. To obtain a good determination of the second contribution, special attention has been devoted to the calculation of the first one, which depends on the strain state and varies with the characteristics of samples. In order to allow a more precise determination of the ZnSe/ZnTe band offset with the tight-binding model, we include (i) a study of earlier and more recent samples over a vast range of different thickness layers and for various strain states; (ii) a study of excited states appearing in transmission spectra; and (iii) the ingredients required to obtain physical parameters, strain properties, and effective masses within the tight-binding framework with spin-orbit interaction. This work is structured as follows. Section II presents the calculation of the electronic transitions. Results are discussed and compared with experiments in Sec. III. This work is concluded in Sec. IV.

II. TIGHT-BINDING CALCULATION

We work in the context of a 20-band tight-binding model including the spin-orbit coupling.[21–23] Our calculations of electronic properties use $sp3s^*$ tight-binding parameters specially chosen so as to reproduce several features of the fundamental properties of bulk constituents. We have generalized their determination in order to extend our method to strained-layer superlattice calculations. For this we have derived some analytical equations relating the effective masses and deformation potentials at the Γ point, and the 15 parameters of the $sp3s^*$ 20-band tight-binding model including spin-orbit coupling. The description of this parametrization for such strained compounds is out of the scope of the present paper, and will be published in a forthcoming paper. Using these relations and other relations between the 15 parameters and Γ and X energy values,[22] we obtain a set of parameters which accurately reproduces the effective masses at Γ, the deformation potentials, and an overall band structure in accordance with reflectivity and photoemission measurements.[24,25] These parameters are given in Table II for ZnTe, and in Ref. 26 for ZnSe. In this table are also given the exponents η_{ij} used for the scaling law[27] which describes the variation of the two-center integrals[28] V_{ij} with respect to the interatomic distance a. $V_{ij}(a)=V_{ij}(a_0/a)^{\eta_{ij}}$, where a_0 is the equilibrium lattice constant. The η_{ij} values are adjusted in order to fit the first pressure derivatives of the E_0, $E_{\Gamma X}$, $E_{\Gamma L}$, E_1, and E_2 transitions. Strain effects upon the electronic structure are taken into account using the Slater-Koster scheme.[28] Table I gives the values of the main physical quantities obtained from tight-binding parameters. Our description ensures the fact that the strain-induced couplings of the light hole with both upper conduction bands and split-off valence band are properly taken into account, and provides a nonlinear variation of band edges with strain. For instance, in the case of ZnSe biaxially strained to ZnTe, this makes a 100-meV nonlinear contribution to the ZnSe light-hole band edge. These facts have been detailed in Refs. 19 and 20.

TABLE II. ZnTe tight-binding parameters (in eV) with the same notation as in Ref. 22, and η_{ij} exponents.

ZnTe					
E_{sa}	−9.658 65	V_{ss}	−4.447 86	$\eta_{ss\sigma}$	4.05
E_{pa}	−0.13601	V_{xx}	1.054 66	$\eta_{pp\sigma}$	3.60
E_{s^*a}	7.0000	V_{xy}	5.000 65	$\eta_{pp\pi}$	0.92
E_{sc}	0.753 15	V_{sapc}	1.548 20	$\eta_{sapc\sigma}$	3.00
E_{pc}	5.644 08	V_{scpa}	5.746 09	$\eta_{scpa\sigma}$	4.00
E_{s^*c}	8.5000	V_{sa^*pc}	3.161 58	$\eta_{s^*apc\sigma}$	2.30
λ_a	0.332 41	V_{sc^*pa}	0.255 98	$\eta_{s^*cpa\sigma}$	2.00
λ_c	0.019 52				

Consider a given [001] $(ZnSe)_m(ZnTe)_n$ superlattice with a well-defined pseudomorphic or free standing strain state. The lattice parameters of the layers are calculated with classical elasticity. From the resulting atomic positions, we can evaluate the matrix elements of the superlattice Hamiltonian at a $\mathbf{k}$ point of the superlattice Brillouin zone. The full diagonalization of the $20(m+n)$ matrix provides the $E(\mathbf{k})$ eigenenergies and the components of eigenfunctions on the 20 $(m+n)$ basis functions. Optical transitions are evaluated with a dipolar approximation along the lines of Ref. 29. In these calculations, we use a non-self-consistent version of the tight-binding model and consequently do not consider the charge distribution at the interface which is important for theoretical calculations of the valence-band offset as in Ref. 11. We have investigated a possible deviation from the macroscopic elasticity at the interface. This does not alter the calculated superlattice energies significantly.

In the previous description, the temperature and the free or bounded excitonic effects are not taken into account, and only 0-K band-to-band transitions are obtained. As the experimental data concerned by this work are spread over a wide temperature range, and as free or bound excitons are present, 0-K calculated transitions have been corrected. The fundamental bulk electronic transition E_0 is known to vary with temperature according to a Varshni law:[30] $E_0(T)=E_0(0)-(\gamma T^2)/(\delta+T)$, γ and δ depending on the compound. For a $(ZnSe)_m(ZnTe)_n$ superlattice, we have corrected our $E(0)$ transitions using an appropriate Varshni law: $E(T)=E(0)-(\bar{\gamma}T^2)/(\bar{\delta}+T)$, where $\bar{\gamma}$ and $\bar{\delta}$ are averages of Varshni empirical parameters for ZnSe and ZnTe:[31]

$$\bar{\gamma}((ZnSe)_m(ZnTe)_n)=\frac{m\gamma_{ZnSe}+n\gamma_{ZnTe}}{m+n}$$

and

$$\bar{\delta}((ZnSe)_m(ZnTe)_n)=\frac{m\delta_{ZnSe}+n\delta_{ZnTe}}{m+n}.$$

Concerning the experimental data at room temperature, we assume the existence of free excitons which reduce the band-to-band transition energy. The value of

the binding energy of the excitons in the superlattices studied is taken from the work of Liu, Rajakarunanayake, and McGill.[32]

III. RESULTS AND DISCUSSION

A. Large-period superlattices

We first considered ZnSe/ZnTe superlattices grown on a GaAs(001) substrate by hot wall epitaxy.[8] Owing to the small value of the crystal thickness due to the large lattice mismatch, these superlattices can be considered in the free-standing approximation because their thickness is large enough to provoke lattice relaxation effects. Raman-scattering measurements carried out on the GaAs substrate and on substrate-free ZnSe/ZnTe superlattices show no Raman shift of the LO-phonon peak and confirm the free-standing state of the layers. Because the ZnTe layers are wider than the ZnSe layers, the in-plane lattice parameter is near the ZnTe one in all the superlattices. We have focused our study on the superlattice consisting of 1.0 nm of ZnSe alternating with 9.0 nm of ZnTe, which corresponds to four and 30 layers of each material, respectively. This configuration has been chosen because its transmission spectra has recently been measured at room temperature and shows some structures in the absorption coefficient curve which correspond to interband transitions including excited states.[8] The valence-band offset is an important parameter to use in determining the superlattice electronic band structure. After some attempts, we used the value deduced from the electronic affinity rule, which corresponds to the best fitting of our results on all the studied samples. Calculations have been carried out using a valence-band-offset value of 1.016 eV. The energy-band lineup is shown in Fig. 2(a). The heavy and light holes are confined in ZnTe layers, whereas electrons are in ZnSe layers leading to a type-II superlattice with spatially indirect electron-hole recombination. In Fig. 3 we represented the probability density of the electronic states lying near the gap in order to analyze their symmetry properties and to investigate the presence of saddle-point excitonic transitions. No mixing exists in the superlattice valence states between the heavy- and light-hole components originating from the bulk states, and the wave functions keep a well-defined parity. The states of the lowest conduction band e_1 are strongly confined in the ZnSe thin layers [Fig. 3(a)] which constitute a 862-meV-deep well. The states of the higher valence band h_1 and l_1 are strongly confined in the ZnTe thick layers [Fig. 3(d)] which constitute a 883-meV-deep well for light-hole states and a 1164-meV-deep well for heavy-hole states. The barrier thickness and the great depth of the wells prevent dispersion along the growth direction k_Z between the states at the center Γ and at the edge Z of the Brillouin zone. As a result the probability density is similar at Γ and Z, although the wave functions at the Γ and Z points have different parities. $e_1(\Gamma)$, $h_1(\Gamma)$, and $l_1(\Gamma)$ states are even with respect to the center of the two layers, the $e_1(Z)$ state is even (odd) with respect to the center of the ZnSe (ZnTe) layers, and the $h_1(Z)$ and $l_1(Z)$ states are even (odd) with respect to the center of the ZnTe (ZnSe) layers. The large well depth wholly confines these states in the wells, and the square of their wave functions is the same at Γ and Z, as can be seen in Figs. 3(a) and 3(d). The $e_2(\Gamma)$ and $e_2(Z)$ states are odd in ZnSe layers and respectively odd and even in ZnTe layers. They are mainly localized in ZnTe layers at the neighboring interfaces. This band lies near the well edge, showing weak dispersion. The next bands are unconfined, and their symmetry properties are different.[33] State $e_3(\Gamma)$ is localized mainly in ZnTe layers. These characteristics allow us to interpret the numerous transitions which occur between the valence and conduction states at Γ and Z points. Results are shown in Fig. 4. Selection rules for confined states allow transitions e_1-h_n with n odd (even) at the Γ (Z) point, and transitions e_2-h_n with n even (odd) at the Γ (Z) point. The lowest conduction states $e_1(\Gamma)$ and $e_1(Z)$ give weak transitions with the upper hole states because electrons are localized in the ZnSe layers, while the hole states are mainly in the ZnTe layers, leading to a type-II structure. More important are the transitions including the second, third, and fourth conduction bands which are wholly or partially localized in the ZnTe layers. Unconfined state symmetry properties enable most of these transitions.[33] Figure 4 clearly indicates that the absorption spectra are first constituted by many weak transitions, giving an absorption curve without well-defined features up to the appearance of the transitions between the valence state h_1 and the e_2, e_3, and e_4 conduction states. As explained in Sec. II, the room-temperature and free-excitonic corrections to be removed from the band-to-band results are 123 and 13 meV, respectively. This gives $e_3-h_1(\Gamma)=2.29$ eV and $e_4-h_2(Z)=2.384$

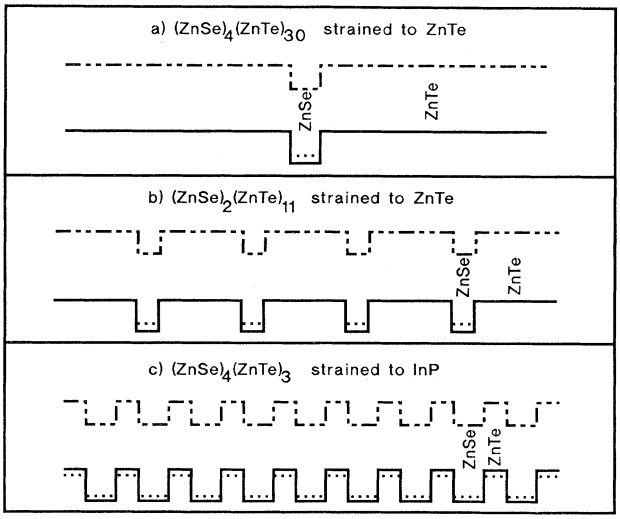

FIG. 2. Band alignment of ZnSe/ZnTe heterostructures in studied configurations. (a) $(ZnSe)_4(ZnTe)_{30}$ superlattice strained to ZnTe lattice parameter. (b) $(ZnSe)_2(ZnTe)_{11}$ superlattices strained to ZnTe lattice parameter. (c) $(ZnSe)_4(ZnTe)_3$ superlattice strained to the InP lattice parameter. In each case, the double-dotted dashed line, dotted line, and full line correspond, respectively, to conduction, light-hole, and heavy-hole states.

eV. The experimental absorption coefficient variation shows two structures at 2.3 and 2.37 eV. These results are in excellent agreement with our theoretical provision of the existence at these energies of two strong structures due to excited electronic states. This interpretation is different from the one proposed in Ref. 8, in which the valence-band offset deduced by fitting to the experimental values is about 0.5 eV, a value which is a great deal smaller than our evaluation of 1.016 eV. However, our value lies in the range of previous estimations proposed by other authors,[1,2,7] and attribution of the absorption threshold to the $e_3-h_1(\Gamma)$ transition allows an interpretation of the optical properties of this sample which is coherent with all other studied samples in this work.

B. Short-period superlattices

We now turn our attention to the ZnSe/ZnTe superlattices grown by MOVPE on a ZnTe buffer deposited onto a (100) GaAs substrate.[9] By using a buffer, coherent growth of superlattices can be expected. However, x-ray-diffraction measurements show that the superlattices are in a free-standing state. Photoluminescence spectra of several samples have been obtained at 2 K. To achieve a better determination of the valence-band offset by fitting to other transitions beside the fundamental gap, we have taken a special interest in the ZnSe/ZnTe superlattice with a period of 4.06 nm because transmission measurements were performed on that sample. Three transitions are detected in the transmission spectra performed at 2K before the onset of absorption at the gap energy of the ZnTe buffer. We have calculated the subband energies using the same value for the valence-band offset as in the previous case (1.016 eV), and assuming that the in-plane lattice parameter $a_{\parallel}$ is equal to (i) the ZnTe lattice parameter (coherent growth) or (ii) the free-standing value. We obtained the same values for the energy states in the two strain configurations. Such a result is easily

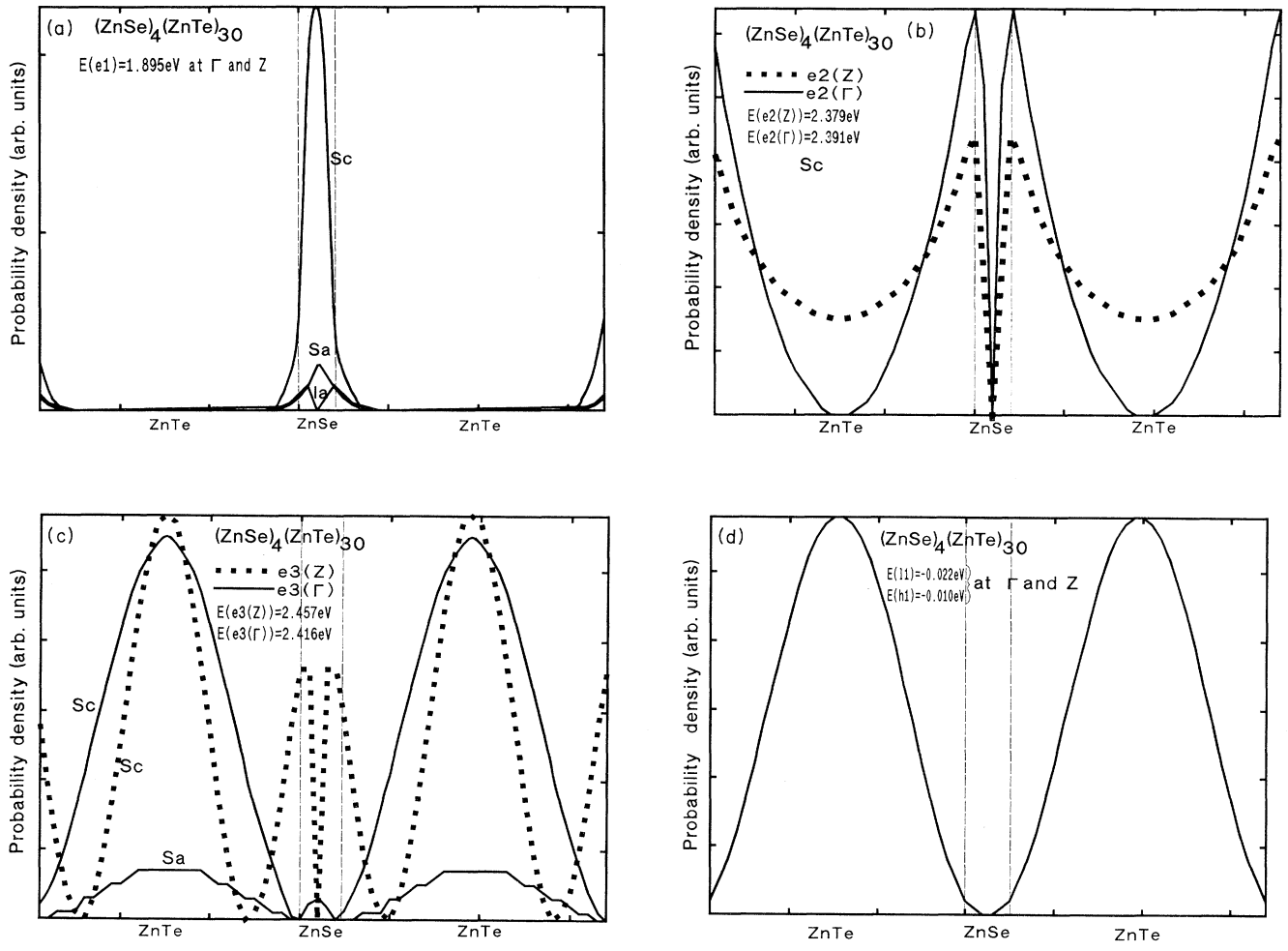

FIG. 3. Contributions of localized orbits to the probability density for the states near the gap vs their positions along the growth axis in the $(ZnSe)_4(ZnTe)_{30}$ superlattice. (a) s-cation, s-anion, and light-hole anion contributions to $e_1(\Gamma)$ and $e_1(Z)$ states. (b) Same as (a) for $e_2(\Gamma)$ and $e_2(Z)$ states, (c) same as (a) for $e_3(\Gamma)$ and $e_3(Z)$ states. (d) Anion contribution to $h_1(\Gamma)$, $h_1(Z)$, $l_1(\Gamma)$, and $l_1(Z)$ states.

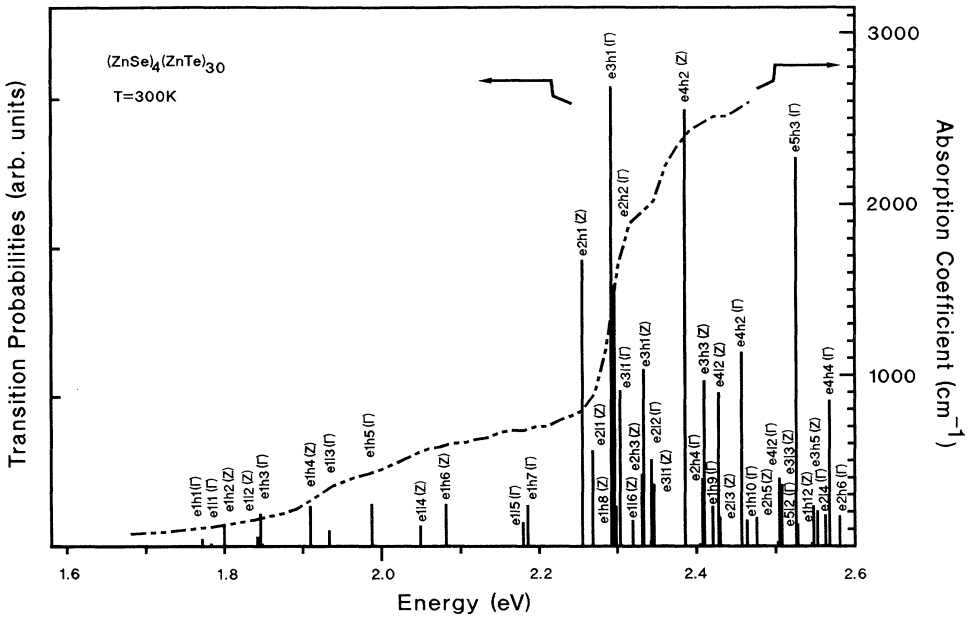

FIG. 4. Lowest-energy transition probabilities (in arbitrary units) for the $(ZnSe)_4(ZnTe)_{30}$ superlattice. The experimental absorption coefficient spectrum of Ref. 8 is reported in comparison.

understood because the ZnTe layer is five times larger than the ZnSe one, leading to very close in-plane lattice parameters. The conduction and valence well depths [Fig. 2(b)] are the same as those in Sec. III A. Figure 5 shows the calculated transition probabilities between the lowest conduction state e_1 and the highest-energy valence states. An excitonic correction of 21 meV (Ref. 32) is done for the three transitions which appear below 2.4 eV. One obtains $e_1-h_1(\Gamma)$ at 2.148 eV, $e_1-l_1(\Gamma)$ at 2.194 eV, and $e_1-h_2(Z)$ at 2.323 eV. This superlattice is of type II as in the previous case. The hole state $h_1(\Gamma)$ remains almost completely localized in the ZnTe layers. Some changes in the electron localization occur. The presence probability of electrons is always maximum in the ZnSe layers; however, the e_1 state extends far from the interfaces, substantially overlapping with the h_1 state in the barrier layers. For this superlattice, the transition probability $e_1-h_1(\Gamma)$ is large and dominates the low-energy range of the absorption spectra, unlike the previous case, for which the large thickness of the barrier strongly reduces the overlap between the two states. In the same figure we report the variation of the absorption coefficient deduced from the transmission spectrum. Three steplike structures are seen in the same energy range and correspond to the first interband transitions. Our theoretical results are in good agreement with this experimental determination, and show that the valence-band-offset value that we have chosen allows correct calculation of the subbands of short-period ZnSe/ZnTe superlattices. Photoluminescence spectra of these ZnSe/ZnTe superlattices present a Stokes shift. This effect can be explained by the trapping of the free exciton at tellurium isoelectronic centers, which is often observed in II-VI compounds.[14] The energy difference between the photoluminescence peak and our band-to-band result is 60 meV, corresponding to excitons bounded on a single isoelectronic Te atom.[14]

C. Very-short-period superlattices

ZnSe/ZnTe superlattices consisting of 1 nm of ZnSe and 1 nm of ZnTe have prompted many studies. The absorption spectrum has been measured at room temperature by Shen[4] on samples prepared by MBE on (100) GaAs or InP substrates. Superlattices with a period of 2 nm have been grown on semi-insulating GaAs(100) surfaces by MBE without any buffer layer, and photoluminescence spectra have been obtained at low temperature by Ozaki[3] for various values of the thickness ratio of the ZnSe layer to the ZnTe one. Photoluminescence spectra of superlattices grown on InP substrates have been obtained by Kobayashi[1] and Dosho[6] on samples

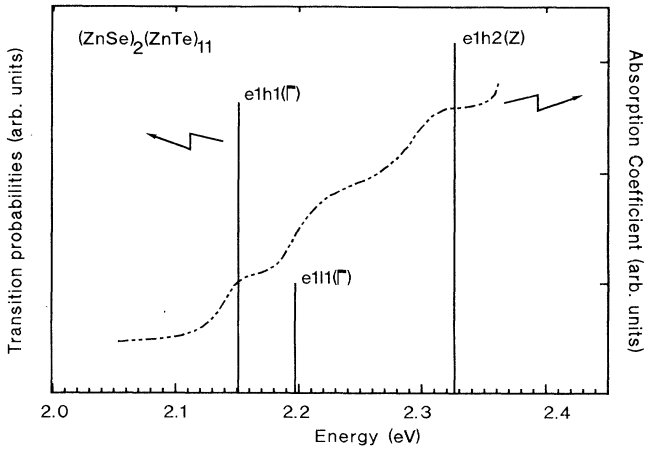

FIG. 5. Lowest-energy transition probabilities (in arbitrary units) for the $(ZnSe)_2(ZnTe)_{11}$ superlattice of Ref. 9. The experimental absorption coefficient spectrum of Ref. 39 is reported in comparison.

grown by ALE. A sample of a period of 1 nm corresponds to 3.53 layers of ZnSe and to 3.28 layers of ZnTe. We have calculated the electronic properties of the superlattice with a unit cell of four layers of ZnSe and three layers of ZnTe, because this is the configuration with an integer number of layers nearest to the nominal structure. The absorption spectrum of 200-period undoped ZnSe/ZnTe superlattices measured by Shen[4] at room temperature shows an absorption threshold at 2.08 eV and an absorption peak at 2.34 eV. Assuming a pseudomorphic superlattice,[6] we calculated the lowest-energy transitions in the optical spectra using the same offset value as above. Here the conduction, light-hole, and heavy-hole well depths values [Fig. 2(c)], respectively, are 836, 755, and 1144 meV. We found the $e_1-h_1(\Gamma)$ band-to-band transition at 2.194 eV and the $e_1-l_1(\Gamma)$ at 2.495 eV. At room temperature, we consider that the excitons are free with a binding energy evaluated to 27 meV by Liu.[32] More important in this experience is the temperature effect that we have estimated to 113 meV following Varshni's expression. If these two corrections are deduced from the theoretical results, at 300 K, we found 2.054 eV for the $e_1-h_1(\Gamma)$ transition and 2.355 eV for the $e_1-l_1(\Gamma)$ transition. These values compare reasonably with the experimental results. These two transitions are the only ones that we have found within the considered spectral domain, and the structures which are experimentally observed between these two values probably do not originate from the interband transitions. A superlattice with similar characteristics has been obtained by epitaxy on a S-doped InP substrate by Kobayashi.[1] The photoluminescence spectra was measured at 71 K for several superlattices with the ZnSe and ZnTe layers of equal thicknesses and different superlattice periods up to 4 nm. The luminescence peak obtained for the sample with 2-nm period lies at 2.01 eV. We have calculated the transition energies for a superlattice with this geometry, pseudomorphically grown onto the InP substrate. We found the transition e_1-h_1 (Γ) at 2.194 eV. Deducing 9 meV for the temperature effect from the theoretical estimation of the band-to-band transition at 0 K gives 2.185 eV. This value is 175 meV, far from the experimental result 2.010 eV at 71 K. This difference agrees with a 170-meV trapping of excitons on Te clusters.[15]

IV. CONCLUSION

We have performed a study of ZnSe/ZnTe superlattices using the tight-binding approximation in order to estimate the valence-band offset considering many experimental studies on a large range of samples with various thicknesses and strain states. The theoretical model uses an $sp3s^*$ basis set with spin-orbit interaction. It enables us to properly describe (i) the whole band structure of ZnTe and ZnSe, (ii) the conduction and valence effective masses, (iii) strain effects on the electronic properties, and (iv) strain-induced band mixings. Energies of superlattice electronic states and optical transition probabilities have been calculated. Excitonic and temperature corrections to band-to-band transition energies have been estimated. We have compared theoretical results with experimental data for large-, short-, and very-short-period ZnSe/ZnTe superlattices. For large-period superlattices, our work shows the important role of unconfined excited states in optical transitions and explains that low-energy structures observed in the absorption spectra are due to transitions between spatially separated conduction and valence superlattice-confined states. The main absorption contribution at higher energy is explained by strong transitions occurring between valence and unconfined conduction states. The features result from the type-II nature of this superlattice. Our calculation leads to a (1.02 ± 0.02)-eV unstrained band offset which allows a very good comparison with the studied experimental data.

ACKNOWLEDGMENTS

We thank the Centre National Universitaire Sud de Calcul (CNUSC Montpellier) for financial support.

[1]M. Kobayashi, N. Mino, H. Katagiri, R. Kimura, M. Konagai, and K. Takahashi, J. Appl. Phys. **60**, 773 (1986); Appl. Phys. Lett. **48**, 296 (1986).

[2]M. Konagai, M. Kobayashi, R. Kimura, and K. Takahashi, J. Cryst. Growth **86**, 290 (1988).

[3]H. Ozaki, K. Imai, and K. Kumazaki, J. Cryst. Growth **127**, 361 (1993).

[4]A. Shen, L. Xu, H. Wang, Y. Chen, and Z. Wang, J. Cryst. Growth **127**, 383 (1993).

[5]T. Yao and T. Takeda, Appl. Phys. Lett. **48**, 160 (1986).

[6]S. Dosho, Y. Takemura, M. Konagai, and K. Takahashi, J. Cryst. Growth **95**, 580 (1989).

[7]H. Kuwabara, H. Fujiyasu, M. Aoki, and S. Yamada, Jpn. J. Appl. Phys. **25**, L707 (1986).

[8]H. Yang, A. Ishida, H. Fujiyasu, and H. Kuwabara, J. Appl. Phys. **65**, 2838 (1989); H. Yang, A. Ishida, and H. Fujiyasu, Appl. Phys. Lett. **56**, 2114 (1990).

[9]N. Briot, T. Cloitre, O. Briot, P. Boring, B. Ponga, B. Gil, R. L. Aulombard, M. Gailhanou, J. M. Sallese, and A. C. Jones, in *Thin Films: Stresses and Mechanical Properties,* edited by P. H. Townsend, T. P. Weihs, J. Sanchez, Jr., and P. Børgesen, MRS Symposia Proceedings No. 308 (Materials Research Society, Pittsburgh, 1993), p. 461.

[10]R. H. Miles, J. O. McCaldin, and T. C McGill, J. Cryst. Growth **85**, 188 (1987).

[11]C. Priester, D. Bertho, and C. Jouanin, Physica B **191**, 1 (1993)

[12]D. Bertho, A. Simon, D. Boiron, C. Jouanin, and C. Priester, J. Cryst. Growth **101**, 372 (1990).

[13]C. Van de Walle, J. Vac. Sci. Technol. B **6**, 1350 (1988).

[14]J. J. Davies, Semicond. Sci. Technol. **3**, 219 (1988).

[15]T. Yao, M. Kato, J. J. Davies, and H. Tanino, J. Cryst. Growth **86**, 552 (1988).

[16]Y. Rajakarunanayake, R. H. Miles, G. Y. Wu, and T. C. McGill, J. Vac. Sci. Technol. B **6**, 1354 (1988); Phys. Rev. B **37**, 10 212 (1988).

[17]Y. Wu, S. Fujita, and S. Fujita, J. Appl. Phys. **67**, 908 (1990).
[18]P. Vogl, H. P. Hjalmarson, and J. D. Dow, J. Phys. Chem. Solids **44**, 365 (1983).
[19]J. M. Jancu, D. Bertho, C. Jouanin, B. Gil, N. Pelekanos, N. Magnea, and H. Mariette, Phys. Rev. B **49**, 10 802 (1994).
[20]D. Bertho, J. M. Jancu, and C. Jouanin, Phys. Rev. B **50**, 16 956 (1994).
[21]P. Vögl, H. P. Hjalmarson, and J. D. Dow, J. Chem. Solids **44**, 365 (1983).
[22]A. Kobayashi, O. F. Sankey, and J. D. Dow, Phys. Rev. B **25**, 6367 (1982).
[23]D. J. Chadi, Phys. Rev. B **16**, 790 (1977).
[24]*Semiconductors, Impurities and Defects in Group IV Elements and III-V Compounds,* edited by O. Madelung, Landolt-Börnstein, New Series, Group III, Vol. 22, Pt. a (Springer-Verlag, Berlin, 1987).
[25]*Semiconductors, Physics of Group IV Elements and III-V Compounds,* edited by O. Madelung, Landolt-Börnstein, New Series, Group III, Vol. 17, Pt. b (Springer-Verlag, Berlin, 1982).
[26]D. Bertho, J. M. Jancu, and C. Jouanin, Phys. Rev. B **48**, 2452 (1993).
[27]W. A. Harrison, *Electronic Structure and the Properties of Solids* (Freeman, San Francisco, 1980).
[28]J. C. Slater and G. F. Koster, Phys. Rev. **94**, 1498 (1954).
[29]L. C. Lew Yan Voon, and L. R. Ram-Mohan, Phys. Rev. B **47**, 15 500 (1993).
[30]Y. P. Varshni, Physica (Utrecht) **34**, 149 (1967).
[31]A. Naumov, H. Stanzl, K. Wolf, S. Lankes, and W. Gebhart, J. Appl. Phys. **74**, 6178 (1993).
[32]Y. X. Liu, Y. Rajakarunanayake, and T. C. McGill, J. Cryst. Growth **117**, 742 (1992).
[33]C. Jouanin, J. M. Jancu, D. Bertho, P. Boring, and B. Gil, Phys. Rev. B **46**, 4988 (1992).
[34]B. Sermage and G. Fishman, Phys. Rev. B **23**, 5107 (1981).
[35]A. A. Kaplyanskii and L. G. Suslina, Fiz. Tverd. Tela (Leningrad) **7**, 2327 (1965) [Sov. Phys. Solid State **7**, 1881 (1966)].
[36]W. Wardzynki, W. Giriat, H. Szynczak, and R. Kowalczyk, Phys. Status Solidi B **49**, 71 (1972).
[37]W. Maier, G. Schmieder, and C. Klingshirn, Z. Phys. B **50**, 193 (1983).
[38]Ch. Neumann, A. Nöthe, and N. O. Lipari, Phys. Rev. B **37**, 922 (1988).
[39]T. Cloitre, N. Briot, O. Briot, P. Boring, B. Gil, and R. L. Aulombard. J. Phys. (France) IV **3**, C5-421 (1993).